Received: 14 December 2018 | Revised: 27 February 2019 | Accepted: 6 March 2019

DOI: 10.1002/jcp.28599

ORIGINAL RESEARCH ARTICLE

WILEY Journal of Cellular Physiology

Combinatorial effects of radiofrequency hyperthermia and radiotherapy in the presence of magneto-plasmonic nanoparticles on MCF-7 breast cancer cells

Fahimeh Hadi[1,2] | Shima Tavakkol[3] | Sophie Laurent[4] | Vahid Pirhajati[3,5] | Seied Rabi Mahdavi[1,6,7] | Ali Neshastehriz[1,2] | Ali Shakeri-Zadeh[1,6,7]

[1]Radiation Biology Research Center, Iran University of Medical Science (IUMS), Tehran, Iran

[2]Radiation Science Department, Iran University of Medical Science (IUMS), Tehran, Iran

[3]Cellular and Molecular Research Center, Iran University of Medical Science (IUMS), Tehran, Iran

[4]General, Organic and Biomedical Chemistry, NMR and Molecular Imaging Laboratory, University of Mons, Mons, Belgium

[5]Neuroscience Research Center, Iran University of Medical Science (IUMS), Tehran, Iran

[6]Finetech in Medicine Research Center, Iran University of Medical Science (IUMS), Tehran, Iran

[7]Medical Physics Department, School of Medicine, Iran University of Medical Science (IUMS), Tehran, Iran

Correspondence
Ali Neshastehriz, PhD, and Ali Shakeri-Zadeh, PhD, Iran University of Medical Sciences, Shahid Hemmat Highway, Tehran 1449614535, Iran.
Email: neshastehriz@yahoo.com (A. N.); shakeriz@iums.ac.ir (A. S.-Z.)

Funding information
Iran University of Medical Sciences

Abstract

Here, the effects of combinatorial cancer therapy including radiotherapy (RT) and radiofrequency (RF) hyperthermia in the presence of gold-coated iron oxide nanoparticles (Au@IONPs), as a thermo-radio-sensitizer, are reported. The level of cell death and the ratio of Bax/Bcl2 genes, involved in the pathway of apoptosis, were measured to evaluate the synergistic effect of Au@IONPs-mediated RF hyperthermia and RT. MCF-7 human breast adenocarcinoma cells were treated with different concentrations of Au@IONPs. After incubation with NPs, the cells were exposed to RF waves (13.56 MHz; 100 W; 15 min). At the same time, thermometry was performed with an infrared (IR) camera. Then, the cells were exposed to 6 MV X-ray at various doses of 2 and 4 Gy. MTT (3-[4,5-dimethylthiazol-2-y1]-2, 5-diphenyltetrazolium bromide) assay was performed to evaluate cell viability and quantitative real-time polymerase chain reaction (qRT-PCR) was used to determine the expression ratio of Bax/Bcl2. Cellular uptake of nanoparticles was confirmed qualitatively and quantitatively. The results obtained from MTT assay and qRT-PCR studies showed that NPs and RF hyperthermia had no significant effect when applied separately, while their combination had synergistic effects on cell viability percentage and the level of apoptosis induction. A synergistic effect was also observed when the cancer cells were treated with a combination of NPs, RF hyperthermia, and RT. On the basis of the obtained results, it may be concluded that the use of magneto-plasmonic NPs in the process of hyperthermia and RT of cancer holds a great promise to develop a new combinatorial cancer therapy strategy.

KEYWORDS
cancer, combination therapy, magneto-plasmonic nanoparticles, radiofrequency hyperthermia, radiotherapy

1 | INTRODUCTION

Breast cancer is one of the most common cancers occurring in women all over the world, with an increasing rate in recent years (Mostafavinia, Khorashadizadeh, & Hoshyar, 2016; A.-W. Zhang et al., 2016). Currently, treatments used for breast cancer are included in surgery, radiation therapy, chemotherapy, and hormone therapy (Song, Cheng, Chao, Yang, & Liu, 2017). In the treatment of breast cancer, radiotherapy (RT) is often done in combination with surgery and mastectomy to reduce the risk of recurrence

(Alizadeh et al., 2019; Shakeri-Zadeh, Eshghi, Mansoori & Hashemian, 2016). Despite many advances in cancer detection and treatment, relapse and metastasis are seen in 40% of patients (Mostafavinia et al., 2016). One of the ways to improve the effectiveness of current treatments is to use various combination therapies (C.-M. Hu, Aryal, & Zhang, 2010). Combination of hyperthermia and RT, called thermo-radiotherapy, increases the destructive effects of ionizing radiations. Tumor temperature rise, leading to both tumor bloodstream enhancement and oxygenation of tumor resistant hypoxic cells, can eliminate cancer cells that are resistant to radiation (Song et al., 2017). Also, it is well-known that hyperthermia disrupts the function of proteins involved in DNA repair (Giustini et al., 2010). In fact, at temperatures above 40°C, the proteins become denatured irreversibly (Mustafa et al., 2013). One of the new methods for noninvasive hyperthermia is the use of electromagnetic waves in the presence of metallic nanoparticles which results in considerable heat generation (Beik et al., 2017). Using radiofrequency (RF) waves with high penetration depth, as a nonionized and nonharmful energy band of electromagnetic spectrum, is highly beneficial to develop a new nanoparticle (NP) mediated hyperthermia procedure (Nasseri, Yilmaz, Turk, Kocum, & Piskin, 2016; Rejinold, Jayakumar, & Kim, 2015). In the process of hyperthermia, it is necessary to only increase the temperature of tumor cells while the temperature of healthy collateral cells must be kept at the normal range (Fazal, Paul-Prasanth, Nair, & Menon, 2017). Because of hysteresis loss or relaxation mechanism, iron oxide nanoparticles (IONPs) can provide substantial heat to eliminate cancer cells when exposed to an alternating magnetic field (Wilhelm, Fortin, & Gazeau, 2007; Zheng et al., 2016). Accordingly, IONPs-mediated hyperthermia provides a novel method for treating deep tumors (Beik, Abed, Ghadimi-Daresajini, et al., 2016; Beik, Abed, Shakeri-Zadeh, Nourbakhsh, & Shiran, 2016; Beik et al., 2017). Also, such a NP can be used as a drug carrier, radiosensitizer, and contrast agent in magnetic resonance imaging (MRI; Eyvazzadeh et al., 2017; Y. Hu et al., 2016; Wilhelm et al., 2007). Uncoated IONPs are accumulated rapidly and absorbed by the macrophages in the body. Therefore, the surface of these NPs should be coated with various materials to minimize the accumulation in physiological conditions (Peng, Qian, Mao, & Wang, 2008). The coating of IONPs with gold can improve their stability and biocompatibility, protect them against chemical reactions, and increase the destructive effects of RT (Fakhimikabir, Tavakoli, Zarrabi, Amouheidari, & Rahgozar, 2018; R. Hu et al., 2017; Mehrnia, Hashemi, Mowla, & Arbabi, 2017). Interaction of ionizing radiations with gold nanoparticle (AuNP), as a high Z material (Z = 79), leads to the production of short-range and low-energy electrons (Compton electron, photo-electron, and Auger electron). As a result, energy absorption inside the cancer cells loaded by AuNPs is significantly increased. In contrast, the collision of X-rays to AuNPs can lead to free radical production so that DNA damage and cell apoptosis can be considered as the main and most important consequences (X. Zhang et al., 2008). Accordingly, AuNPs can be utilized as a radiosensitizer in the process of cancer RT (Darfarin et al., 2018; Ghaznavi et al., 2018; Shakeri-Zadeh et al., 2014).

In this study, we investigated the potentials of magneto-plasmonic core-shell nanocomplex made of gold-coated iron oxide nanoparticles (Au@IONPs) when applied in the process of combinatorial RF hyperthermia and RT of cancer. We studied the effects of such a combinatorial treatment on MCF-7 human breast adenocarcinoma cells and closely looked at the level of cell death and the expression of apoptotic genes in different treatment groups.

2 | MATERIALS AND METHODS

2.1 | Cell culture

MCF-7 cell line was prepared from the Pasteur Institute (Tehran, Iran) and cultured in Dulbecco's modified Eagle's medium F-12 (DMEM F-12) supplemented with 1% penicillin–streptomycin (Sigma-Aldrich, St Louis, MO) and 10% fetal bovine serum (FBS; Gibco, Grand Island, NY) at 37°C in an atmosphere of 5% CO_2 incubator. Cells were subcultured using trypsin–ethylenediaminetetraacetic acid (EDTA; Sigma-Aldrich).

2.2 | Synthesis and characterization of Au@IONP core-shell NPs

Au@IONPs core-shell NPs were synthesized as reported previously (Kang, Risbud, Rabolt, & Stroeve, 1996; Mirrahimi et al., 2018). In brief, such a core-shell NP was synthesized through the deposition of AuNPs on Fe_2O_3 NPs using the modified Lyon's iterative hydroxylamine-seeding procedure (Lyon, Fleming, Stone, Schiffer, & Williams, 2004). The morphology and size distribution of NPs, were determined using a Zeiss LEO 906 transmission electron microscopy (TEM). The hydrodynamic diameter of the NPs and their surface charge were measured using the Malvern Zetasizer Nano ZS-90 instrument.

2.3 | Cytotoxicity of the Au@IONPs core-shell NPs

Cytotoxicity of the synthesized core-shell NPs was evaluated on MCF-7 cells using MTT (3-[4, 5-dimethylthiazol-2-y1]-2, 5-diphenyl-tetrazolium bromide; Sigma-Aldrich) assay. Cells were seeded into 96-well plates at a density of 10,000 cells/well in 100 µl of cell culture medium and incubated for 24 hr. Then, 100 µl media with different concentrations of Au@IONP nanocomplex (0, 5, 10, 15, 20, 25, and 30 µg/ml) were added to the cells instead of the initial medium. After 4 hr, cells were washed with phosphate-buffered saline (PBS) add fresh medium was added to each well. Treated cells were returned to the incubator and kept overnight. Then, the medium was removed and 100 µl MTT solution (5 mg/ml in PBS) was added to each well and plates were incubated 4 hr at 37°C. Then, MTT solution was removed and 100 µl dimethylsulfoxide (DMSO) was added to each well and the absorbance of wells measured by enzyme-linked immunosorbent assay (ELISA) reader at 570 nm. The cell survival rate for different groups was calculated in comparison with the control group.

2.4 | Cellular uptake experiments

Such investigations were done using two different methods; inductively coupled plasma mass spectrometry (ICP-MS) and transmission electron microscopy (TEM). MCF-7 cells were cultured in two wells of six-well plates (300,000 cells/well). After 24 hr, 1 ml of medium with NPs concentration of 20 μg/ml was added to each well and the cells were incubated for 4 hr. Then, the cells were washed with PBS, collected using trypsin, and finally centrifuged. In this step, two separate cell pellets were obtained. One of the cell pellets was dissolved in aqua regia and examined for the Au content by ICP-MS (ELAN DRC-e spectrometer; PerkinElmer SCIEX, Concord, Ontario, Canada). Another sample of cell pellet was fixed with glutaraldehyde fixative and was examined by TEM to visualize the process of NPs cellular uptake.

2.5 | Thermometry

The effects of NPs on temperature rise profile of the MCF-7 cells irradiated by RF waves were also evaluated. The cells were cultured in two separate T12 culture flasks. After 24 hr, the cells inside the first flask was incubated with NPs (20 μg/ml) for 4 hr at 37°C. Then, the cells impregnated by NPs were washed with PBS and fresh medium was added. The second T12 flask received no NPs. Both samples, with and without NPs, were exposed to RF waves (100 W, 13.56 MHz, Basafan, Tehran, Iran). The temperature of cells was monitored and measured every 2 min by IR camera (Testo 875–1i; Lenzkirch, Germany).

2.6 | Combination treatment

MCF-7 cells were seeded in four-well plates (60,000 cells/well). After 24 hr, cells were treated with 300 μl NP_s (20 μg/ml) and incubated for 4 hr at 37°C. Then, the cells were washed with PBS and fresh medium was added. Samples were exposed to RF waves at the power of 100 W for 15 min. After an hour, cells were exposed to different doses of 6-MV X-ray radiation (2 and 4 Gy) and then returned to the incubator. After 24 hr, the medium was removed and 300 μl MTT solution was added to each well and plates were incubated for 4 hr at 37°C. Then, MTT solution was removed and 300 μl DMSO was added to each well and then the purple solution of each group was separately transferred to the rows of a 96-well microplate (100 μl/well). The absorbance of wells was measured by ELISA reader (Dynex MRX, Dynex Technologies Inc., Chantilly, VA) at 570 nm. The cell survival rate of different groups was calculated in comparison with control group. MTT assay was done 24 hr posttreatment since the doubling time of MCF-7 cells was obtained at 24:07 hr in our lab. Accordingly, we performed such an assay 24 hr posttreatments to evaluate the effects after one doubling time.

2.7 | Quantitative real-time polymerase chain reaction (qRT-PCR)

After treatment of cells with RF hyperthermia and RT in the presence of NPs, expression changes for two genes involved in the apoptosis pathway (Bax and Bcl2) were investigated. The cells (500,000) were cultured in T12 culture flask and different treatments were applied, as described in Section 2.6. The cells were collected and centrifuged after each treatment and total RNA was extracted using RNX-Plus Solution Kit (SinaClon, Tehran, Iran). Concentration and purity of RNA were determined by measuring the absorbance of the samples at 260 and 280 nm by using NanoDrop (Thermo Fisher Scientific, Waltham, MA). After RNA extraction, complementary DNA (cDNA) was synthesized using Takara cDNA Synthesis Kit (Takara, Burlington, Japan). RT-PCR was performed by Rotor-Gene Q Real-Time Analyzer (Corbett, Sydney, Australia) using EvaGreen Master Mix (Solis BioDyne, Estonia). Forward and reverse primers used in this study are listed in Table 1. Gene expression level was quantified using the $\Delta\Delta C_t$ method. The β-actin was utilized for normalization the relative level of gene expression. Similar to MTT assay, RT-PCR test was also done 24 hr posttreatment with regard to MCF-7 doubling time.

2.8 | Statistical analysis

Statistical analysis was performed using the GraphPad Prism 6 software (GraphPad Software, Inc., San Diego, CA). One way analysis of variance test was used to evaluate the significance of results. A value of $p < 0.05$ was considered statistically significant.

3 | RESULTS

Figure 1 shows TEM images of Au@IONPs core-shell nanocomplex. The core-shell structure and spherical shape are observed. Moreover, Figure 2a shows the hydrodynamic size distribution of the synthesized NPs reporting that the NPs size was ranged from 20 to 40 nm (peak: 30.3 nm). Also, Zeta potential analysis showed the synthesized NPs were negatively charged (−34.1 mV), indicating good stability of NPs (Figure 2b).

Figure 3 shows the results of MTT assay conducted to determine the cytotoxic effects of NPs at various concentrations. Results

TABLE 1 Primer sequences of the genes used for qRT-PCR experiments in this study

Genes	Forward primer	Reverse primer
Bax	CAACTGGTGCTCAAGGCC	GAGACAGGACATCAGTC
Bcl2	TGGAGAGTGCTGAAGATTGATG	AGTCTACTTCCTCTGTGATGTTG
β-Actin	TGAAGATCAAGATCATTGCTCCTC	TCAGTAACAGTCCGCCTAGAAG

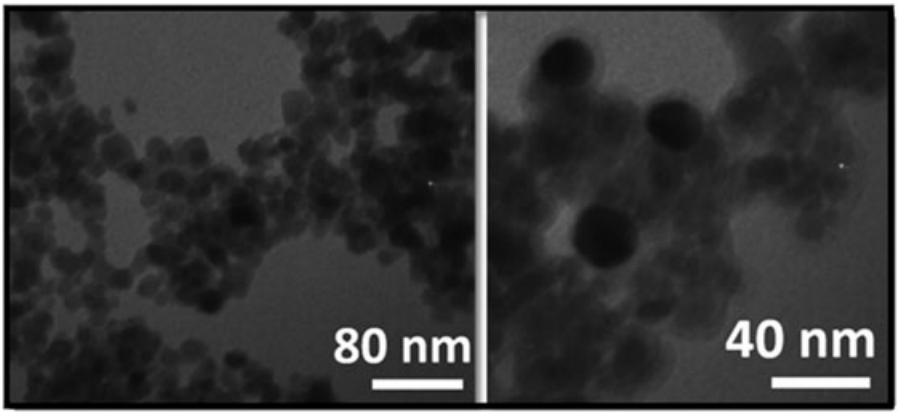

FIGURE 1 Transmission electron microscopy images of the synthesized Au@IONPs core-shell NPs. Au@IONP: gold-coated iron oxide nanoparticle; NP: nanoparticle

indicated that after 4 hr incubation of NPs (20 μg/ml) with the MCF-7 cells, their viability was 87.5% and NPs had no significant cytotoxicity at this concentration ($p > 0.05$). According to this result, we selected 20 μg/ml as the concentration for further studies (e.g., cell uptake tests and combinatorial cancer therapy experiments).

TEM images presented in Figure 4 indicate the uptake process of NPs into MCF-7 cells mitochondria and cytoplasm. ICP-MS measurements also confirmed the presence of nanoparticles into the cells by determination of the Au content. We observed that 0.1 ng of Au was entered into each cell following the incubation of NPs with MCF-7 cells.

Before conducting any further experiments in the field of hyperthermia, we needed to know the effects of NPs on the temperature profile of MCF-7 cells exposed by RF waves. Our thermometry studies indicated that the temperature of the MCF-7 cells loaded by NPs and exposed by RF exposure reached 43.1°C. This is while the NPs free cells experienced 39°C when the similar condition of RF exposure was applied. The results of MTT assay for the MCF-7 cells received NPs alone, RF waves alone and the combination of NPs + RF are presented in Figure 5. As seen in this figure, RF waves or NPs did not induce any significant cell death when applied alone ($p > 0.05$). Cell survival rate was 88.99% and 87.50% for RF and NPs group, respectively. This is while the combination of NPs and RF hyperthermia reduced cell survival rate to 57.37% ($p < 0.0001$ in comparison with the control group).

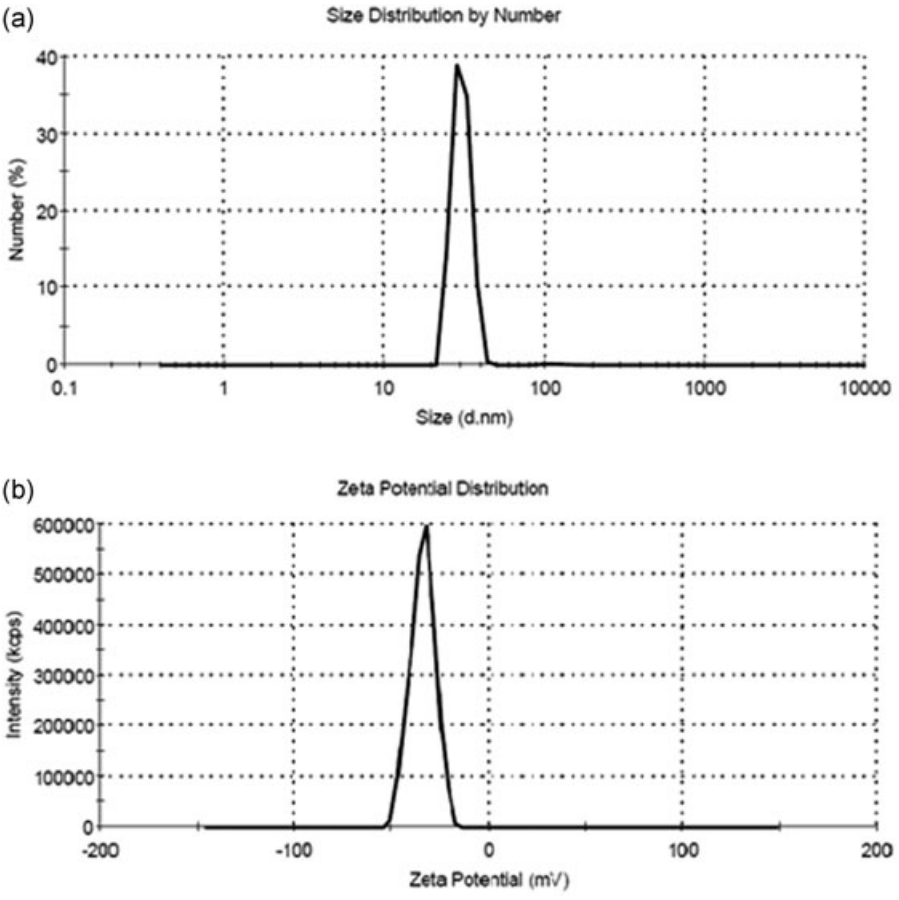

FIGURE 2 (a) Hydrodynamic size and (b) Zeta potential distribution of the synthesized Au@IONPs core-shell NPs. Au@IONP: gold-coated iron oxide nanoparticle; NP: nanoparticle

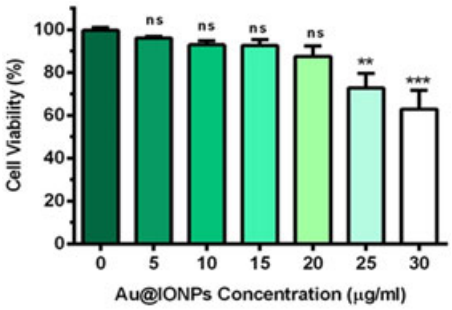

FIGURE 3 The viability of MCF-7 cells treated with different concentrations of Au@IONPs core-shell NPs for 4 hr (*ns* stands for not statistically significant, $^{**}p < 0.01$, $^{***}p < 0.001$ when each experimental group was compared with its corresponding control group). Au@IONP: gold-coated iron oxide nanoparticle; NP: nanoparticle [Color figure can be viewed at wileyonlinelibrary.com]

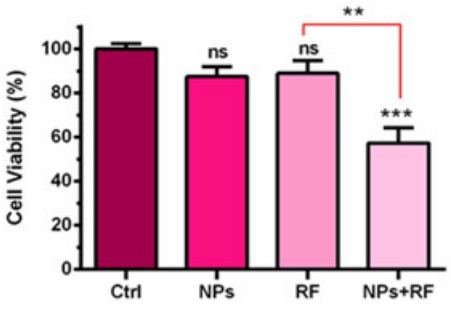

FIGURE 5 The viability of MCF-7 cells treated with NPs alone, RF waves alone and the combination of NPs + RF hyperthermia (*ns* stands for not statistically significant, $^{**}p < 0.01$ and $^{***}p < 0.001$ when each experimental group was compared with its corresponding control group). NP: nanoparticle; RF: radiofrequency [Color figure can be viewed at wileyonlinelibrary.com]

Figure 6 shows the viability of MCF-7 cells after radiation therapy with and without NPs. When RT was performed in the presence of NPs, cell survival was reduced from 86.32% to 70.44% and from 77.50% to 57.28% for 2 and 4 Gy, respectively. Finally, the combinatorial effects of RF hyperthermia and RT with and without NPs were studied on MCF-7 cells to determine whether or not such combination therapy has any synergistic effects. Figure 7 shows the results of this section of the present study, demonstrating a significant difference between two RF + RT groups with and without NPs ($p < 0.05$).

In another step of this study, Bax and Bcl-2 genes expression levels were determined for various experimental groups and then the ratio of Bax/Bcl-2 was calculated. Such a ratio represents the occurrence of apoptosis in each treatment group. As mentioned before, β-actin gene was considered as the house-keeping gene. The relative changes in Bax/Bcl-2 ratio for various experimental groups are shown in Figure 8. According to this figure, Bax/Bcl-2 ratio in the groups received a single treatment modality did not have a significant difference with the control group ($p > 0.05$) except for 4 Gy-RT, but the combination of NPs with RT and RF made a significant difference and increased the Bax/Bcl-2 ratio. After combining the [NPs + RF] treatment modalities with RT, there was no significant difference between the group received 2 and 4 Gy radiation. In other words, in such a combination therapy, lower dose of RT has the results similar to what obtained for the greater doses.

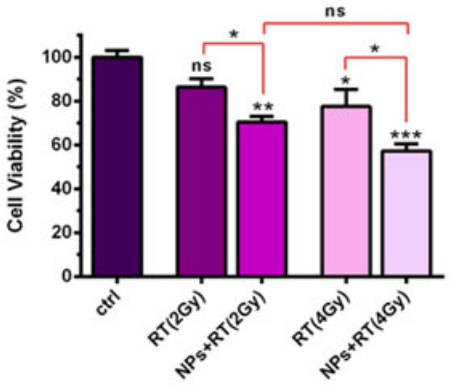

FIGURE 6 The viability of MCF-7 cells treated with NPs and then exposed to different doses of X-ray radiation (*ns* stands for not statistically significant, $^{*}p < 0.05$, $^{**}p < 0.01$, and $^{***}p < 0.001$ when each experimental group was compared with its corresponding control group) [Color figure can be viewed at wileyonlinelibrary.com]

4 | DISCUSSION

Radiation therapy is one of the main treatment methods for cancer and in many cases, it is used as a supportive treatment (Schaue & McBride, 2015). The efficacy of RT can be increased if combined with hyperthermia (Overgaard, 2013). In this study, we aimed to evaluate the synergistic effect of NPs-mediated thermo-radiotherapy on breast cancer cells. To

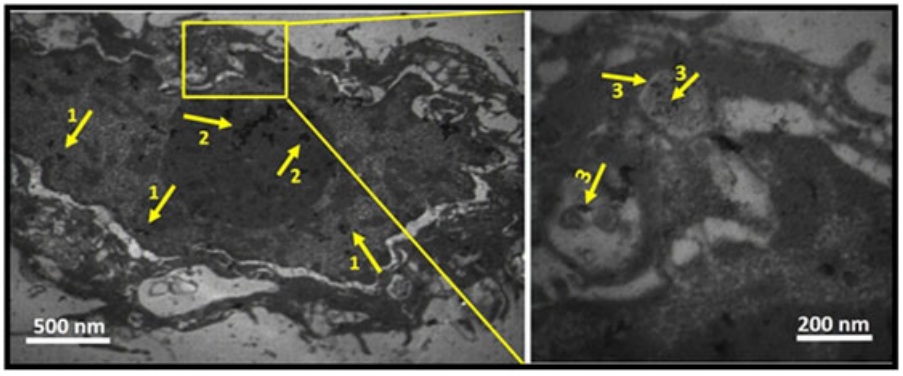

FIGURE 4 Cellular uptake assay for the Au@IONPs core-shell NPs, after 4 hr incubation. Yellow arrows show nanoparticles inside the (1) cytoplasm and (2) nucleus, and (3) mitochondria. Au@IONP: gold-coated iron oxide nanoparticle; NP: nanoparticle [Color figure can be viewed at wileyonlinelibrary.com]

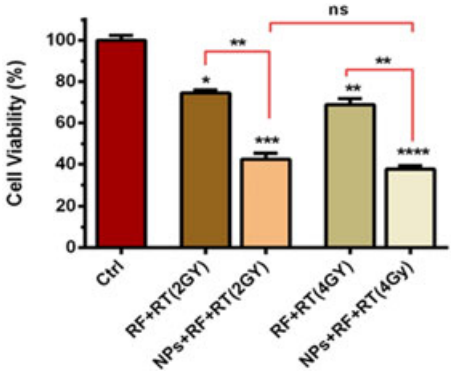

FIGURE 7 The viability of MCF-7 cells after receiving various combination therapy (*ns* stands for not statistically significant, $^{*}p < 0.05$, $^{**}p < 0.01$, $^{***}p < 0.001$, and $^{****}p < 0.0001$ when each experimental group was compared with its corresponding control group) [Color figure can be viewed at wileyonlinelibrary.com]

this end, the magneto-plasmonic Au@IONPs nanocomplex was selected because of good stability, biocompatibility, and multifunctionality, as described in Section 1 (Alizadeh et al., 2019; Chung & Shih, 2014; Eyvazzadeh et al., 2017; Hashemian, Eshghi, Mansoori, Shakeri-Zadeh, & Mehdizadeh, 2009). After synthesis of NPs, we characterized them using various methods. The TEM images showed a core-shell nanostructure for the synthesized NPs with an average diameter of 30 nm. Zeta potential analysis showed that the synthesized NPs was negative (−34 mV), indicating good colloidal stability (Spirou et al., 2018). Since biocompatibility is the main prerequisite for the clinical application of a nanomaterial (Chen et al., 2012), cytotoxicity of the synthesized NPs was evaluated. MTT assay showed that the synthesized Au@IONPs has no cytotoxic effects on MCF-7 cells, when the NPs concentrations lower than 20 μg/ml were utilized. Manjili, Naderi-Manesh, Mashhadikhan, Ma'mani, and Nikzad (2014) also reported approximately similar results.

In thermometry studies, we observed that NPs containing cells had a higher temperature than the cells without NPs if similarly exposed to RF waves. In 2013, Nasseri et al. (2016) reported the temperature rise profile of the samples containing IONPs, Au@IONPs, and AuNPs when exposed to RF waves. Highest temperature was observed for the samples containing IONPs and Au@IONPs. Accordingly, it can be stated that our results are in agreement with what reported by Nasseri et al. (2016).

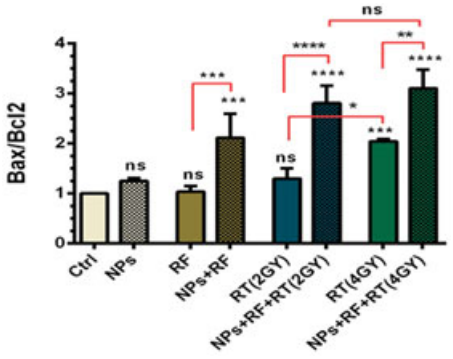

FIGURE 8 The ratio of Bax/Bcl-2 in MCF-7 cells after various combination therapy modalities (*ns* stands for not statistically significant, $^{**}p < 0.01$, $^{***}p < 0.001$, $^{****}p < 0.0001$ when each experimental group was compared with its corresponding control group) [Color figure can be viewed at wileyonlinelibrary.com]

We also observed that the presence of Au@IONPs in the cancer cells enhanced the effects of RF waves and cell death changed from ~11% to ~43% (see Figure 5). Moreover, Bax/Bcl-2 ratio was almost doubled when the cells were treated by the combination of NPs and RF waves, indicating the occurrence of apoptosis was increased during such a NPs-mediated hyperthermia process (see Figure 8). In 2018, Kumar, Chauhan, Jha, & Kuanr (2018) also reported the combined effects of graphene oxide-iron oxide ($GOFe_3O_4$) nanocomposite and RF hyperthermia therapy on A549 human lung epithelial adenocarcinoma cells. The results of their work showed that the presence of such NPs in the cancer cells significantly increased both the cell temperature and cell death after RF exposure.

It is well-known that hyperthermia is able to sensitize the radioresistant cancer cells (Thapa et al., 2015). Accordingly, we evaluated the combined effects of RF hyperthermia and RT in the presence of Au@IONPs in cancer cells. The results showed that the cell death increased significantly and reached 58% for NPs + RF + RT (2 Gy) and 63% for NPs + RF + RT(4 Gy) treatment modalities (Figure 7). Also, Bax/Bcl-2 ratio was almost tripled in these treatment groups (Figure 8). By looking at both Figures 7 and 8, the synergistic effects can be seen for NPs + RF + RT treatment modalities. In 2018, our research team evaluated the combinatorial effects of two methods of hyperthermia (water bath and laser) with RT in the presence of Au@IONPs core-shell NPs inside cancer cells. The results in both studies indicated that, despite the use of different hyperthermia methods, the combination of (NPs + hyperthermia + RT) had a synergistic effect on cell death and apoptosis (Farashahi et al., 2019; Hosseini et al., 2018). Simultaneous use of hyperthermia and RT may cause the intensification of free radical function and production of intracellular reactive oxygen species (ROS), leading to trigger the apoptosis in cancer cells (Abdal Dayem et al., 2017; Fu et al., 2017; Jabbari, Zarei, Esmaeili Govarchin Galeh, & Mansori Motlagh, 2018). Also, we recently studied the ultrastructural features change of a cancer cell due to treatment with (NPs + Hyperthermia + RT) regimen (Movahedi et al., 2018). We observed that the cells treated with a combination of gold nanorods, laser and X-rays experience significant damages, such as plasma membrane blebbing and chromatin condensation as the typical morphological characteristics of apoptosis. Moreover, we observed that autophagic vacuoles can be easily detected in a cancer cell treated by such a combinatorial treatment modality. Accordingly, it is expectable that the treatment of MCF-7 cells with suggested combinatorial treatment modality (core-shell NPs, RF waves, and RT) may also induce massive cell injury so that the main consequence can appear as the cell apoptosis.

5 | CONCLUSIONS

In this study, we investigated the potentials of Au@IONPs when applied in the process of combinatorial hyperthermia and ionizing radiation

therapy of cancer. Our findings demonstrated: (a) Au@IONPs and RF hyperthermia had no significant effect when applied separately, but their combination had a synergistic effect on cell viability, (b) the combination of RT with RF hyperthermia or with NPs significantly enhanced the effects of RT, and (c) a synergistic effect was observed when the Au@IONPs, RF hyperthermia, and RT were combined and applied to the cancer cells altogether. On the basis of the obtained results, it may be concluded that the use of magneto-plasmonic NPs in the process of hyperthermia and RT of cancer holds a great promise to develop a new combinatorial cancer therapy strategy.

ACKNOWLEDGMENT

All financial supports received from IUMS are acknowledged.

CONFLICT OF INTERESTS

The authors declare that there are no conflict of interests.

AUTHOR CONTRIBUTIONS

F. H., A. N., S. T., and A. S.-Z. have made substantial contributions to conception and design, acquisition of data, analysis and interpretation of data, and finally manuscript preparation. V. P. did TEM studies and prepared the draft of manuscript describing the results obtained in TEM studies. S. L. was the advisor of this project for nanoparticles synthesis and she has been involved in drafting and revising the manuscript. S. R. M. was the advisor of this project in the field of radiotherapy and he has been involved in drafting and revising the manuscript.

ORCID

Shima Tavakkol http://orcid.org/0000-0002-8531-7650
Ali Shakeri-Zadeh http://orcid.org/0000-0002-2847-9223

REFERENCES

Abdal Dayem, A., Hossain, M., Lee, S., Kim, K., Saha, S., Yang, G.-M., … Cho, S.-G. (2017). The role of reactive oxygen species (ROS) in the biological activities of metallic nanoparticles. *International Journal of Molecular Sciences*, *18*(1), 120.

Alizadeh, R., Bagher, Z., Kamrava, S. K., Falah, M., Hamidabadi, H. G., Boroujeni, M., … Olya, A. (2019). Differentiation of human mesenchymal stem cells (MSC) to dopaminergic neurons: A comparison between Wharton's jelly and olfactory mucosa as sources of MSCs. *Journal of Chemical Neuroanatomy*, *96*, 126–133.

Beik, J., Abed, Z., Ghadimi-Daresajini, A., Nourbakhsh, M., Shakeri-Zadeh, A., Ghasemi, M. S., & Shiran, M. B. (2016). Measurements of nanoparticle-enhanced heating from 1 MHz ultrasound in solution and in mice bearing CT26 colon tumors. *Journal of Thermal Biology*, *62*, 84–89.

Beik, J., Abed, Z., Shakeri-Zadeh, A., Nourbakhsh, M., & Shiran, M. B. (2016). Evaluation of the sonosensitizing properties of nano-graphene oxide in comparison with iron oxide and gold nanoparticles. *Physica E: Low-dimensional Systems and Nanostructures*, *81*, 308–314.

Beik, J., Khademi, S., Attaran, N., Sarkar, S., Shakeri-Zadeh, A., Ghaznavi, H., & Ghadiri, H. (2017). Nanotechnology based strategy to increase the efficiency of cancer diagnosis and therapy: Folate conjugated gold nanoparticles. *Current Medicinal Chemistry*, *24*(39), 4399–4416.

Chen, D., Tang, Q., Li, X., Zhou, X., Zang, J., Xue, W.-Q., … Guo, C.-Q. (2012). Biocompatibility of magnetic Fe3O4 nanoparticles and their cytotoxic effect on MCF-7 cells. *International Journal of Nanomedicine*, *7*, 4973.

Chung, R.-J., & Shih, H.-T. (2014). Preparation of multifunctional Fe@ Au core-shell nanoparticles with surface grafting as a potential treatment for magnetic hyperthermia. *Materials*, *7*(2), 653–661.

Darfarin, G., Salehi, R., Alizadeh, E., Nasiri Motlagh, B., Akbarzadeh, A., & Farajollahi, A. (2018). The effect of SiO2/Au core–shell nanoparticles on breast cancer cell's radiotherapy. *Artificial Cells Nanomedicine, and Biotechnology*, *46*(Suppl. 2), 836–846.

Eyvazzadeh, N., Shakeri-Zadeh, A., Fekrazad, R., Amini, E., Ghaznavi, H., & Kamrava, S. K. (2017). Gold-coated magnetic nanoparticle as a nanotheranostic agent for magnetic resonance imaging and photothermal therapy of cancer. *Lasers in Medical Science*, *32*(7), 1469–1477.

Fakhimikabir, H., Tavakoli, M. B., Zarrabi, A., Amouheidari, A., & Rahgozar, S. (2018). Could FA-PG-SPIONs act as a hyperthermia sensitizing agent? An in vitro study. *Journal of Thermal Biology*, *78*, 73–83.

Farashahi, A., Zare-Sadeghi, A., Shakeri-Zadeh, A., Kamrava, S. K., Maleki, S., Ghaznavi, H., & Faeghi, F. (2019). Real-time mapping of heat generation and distribution in a laser irradiated agar phantom loaded with gold nanoparticles using MR temperature imaging. *Photodiagnosis and Photodynamic Therapy*, *25*, 66–73.

Fazal, S., Paul-Prasanth, B., Nair, S. V., & Menon, D. (2017). Theranostic iron oxide/gold ion nanoprobes for MR imaging and noninvasive RF hyperthermia. *ACS Applied Materials & Interfaces*, *9*(34), 28260–28272.

Fu, Q., Huang, T., Wang, X., Lu, C., Liu, F., Yang, G., … Wang, B. (2017). Association of elevated reactive oxygen species and hyperthermia induced radiosensitivity in cancer stem-like cells. *Oncotarget*, *8*(60), 101560.

Ghaznavi, H., Hosseini-Nami, S., Kamrava, K., Irajirad, R., Maleki, S., Shakeri-Zadeh, A., & Montazerabadi, A. (2018). Folic acid conjugated PEG coated gold–iron oxide core–shell nanocomplex as a potential agent for targeted photothermal therapy of cancer . *Artificial Cells, Nanomedicine, and Biotechnology*, *46*(8), 1594–1604.

Giustini, A. J., Petryk, A. A., Cassim, S. M., Tate, J. A., Baker, I., & Hoopes, P. J. (2010). Magnetic nanoparticle hyperthermia in cancer treatment. *Nano Life*, *1*(01n02), 17–32.

Hashemian, A. R., Eshghi, H., Mansoori, G. A., Shakeri-Zadeh, A., & Mehdizadeh, A. R. (2009). Folate-conjugated gold nanoparticles (synthesis, characterization and design for cancer cells nanotechnology-based targeting). *International Journal of Nanoscience and Nanotechnology*, *5*(1), 25–34.

Hosseini, V., Mirrahimi, M., Shakeri-Zadeh, A., Koosha, F., Ghalandari, B., Maleki, S., … Kamrava, S. K. (2018). Multimodal cancer cell therapy using Au@ Fe2O3 core–shell nanoparticles in combination with photo-thermo-radiotherapy. *Photodiagnosis and Photodynamic Therapy*, *24*, 129–135.

Hu, C.-M., Aryal, S., & Zhang, L. (2010). Nanoparticle-assisted combination therapies for effective cancer treatment. *Therapeutic Delivery*, *1*(2), 323–334.

Hu, R., Zheng, M., Wu, J., Li, C., Shen, D., Yang, D., … Dong, W. (2017). Core-shell magnetic gold nanoparticles for magnetic field-enhanced radio-photothermal therapy in cervical cancer. *Nanomaterials*, *7*(5), 111.

Hu, Y., Wang, R., Wang, S., Ding, L., Li, J., Luo, Y., … Shi, X. (2016). Multifunctional Fe_3O_4@ Au core/shell nanostars: A unique platform for multimode imaging and photothermal therapy of tumors. *Scientific Reports*, *6*, 28325.

Jabbari, N., Zarei, L., Esmaeili Govarchin Galeh, H., & Mansori Motlagh, B. (2018). Assessment of synergistic effect of combining hyperthermia with irradiation and calcium carbonate nanoparticles on proliferation

of human breast adenocarcinoma cell line (MCF-7 cells). *Artificial Cells, Nanomedicine, and Biotechnology*, *46*, 364–372.

Kang, Y. S., Risbud, S., Rabolt, J. F., & Stroeve, P. (1996). Synthesis and characterization of nanometer-size Fe_3O_4 and γ-Fe_2O_3 particles. *Chemistry of Materials*, *8*(9), 2209–2211.

Kumar, R., Chauhan, A., Jha, S. K., & Kuanr, B. K. (2018). Localized cancer treatment by radio-frequency hyperthermia using magnetic nanoparticles immobilized on graphene oxide-from novel synthesis to in-vitro studies. *Journal of Materials Chemistry B*, *6*, 5385–5399.

Lyon, J. L., Fleming, D. A., Stone, M. B., Schiffer, P., & Williams, M. E. (2004). Synthesis of Fe oxide core/Au shell nanoparticles by iterative hydroxylamine seeding. *Nano Letters*, *4*(4), 719–723.

Manjili, H. K., Naderi-Manesh, H., Mashhadikhan, M., Ma'mani, L., & Nikzad, S. (2014). The effect of iron-gold core shell magnetic nanoparticles on the sensitization of breast cancer cells to irradiation. *Journal of Paramedical Sciences*, *5*(2), 85–90.

Mehrnia, S. S., Hashemi, B., Mowla, S. J., & Arbabi, A. (2017). Enhancing the effect of 4MeV electron beam using gold nanoparticles in breast cancer cells. *Physica Medica*, *35*, 18–24.

Mirrahimi, M., Hosseini, V., Kamrava, S. K., Attaran, N., Beik, J., Kooranifar, S., … Shakeri-Zadeh, A. (2018). Selective heat generation in cancer cells using a combination of 808 nm laser irradiation and the folate-conjugated Fe_2O_3@ Au nanocomplex. *Artificial Cells, Nanomedicine, and Biotechnology*, *46*, 241–253.

Mostafavinia, S. E., Khorashadizadeh, M., & Hoshyar, R. (2016). Antiproliferative and proapoptotic effects of crocin combined with hyperthermia on human breast cancer cells. *DNA and Cell Biology*, *35*(7), 340–347.

Movahedi, M. M., Mehdizadeh, A., Koosha, F., Eslahi, N., Mahabadi, V. P., Ghaznavi, H., & Shakeri-Zadeh, A. (2018). Investigating the photo-thermo-radiosensitization effects of folate-conjugated gold nanorods on KB nasopharyngeal carcinoma cells. *Photodiagnosis and Photodynamic Therapy*, *24*, 324–331.

Mustafa, T., Zhang, Y., Watanabe, F., Karmakar, A., Asar, M. P., Little, R., … Biris, A. S. (2013). Iron oxide nanoparticle-based radio-frequency thermotherapy for human breast adenocarcinoma cancer cells. *Biomaterials Science*, *1*(8), 870–880.

Nasseri, B., Yilmaz, M., Turk, M., Kocum, I. C., & Piskin, E. (2016). Antenna-type radiofrequency generator in nanoparticle-mediated hyperthermia. *RSC Advances*, *6*(54), 48427–48434.

Overgaard, J. (2013). The heat is (still) on—The past and future of hyperthermic radiation oncology. *Radiotherapy and Oncology*, *109*(2), 185–187.

Peng, X.-H., Qian, X., Mao, H., & Wang, A. Y. (2008). Targeted magnetic iron oxide nanoparticles for tumor imaging and therapy. *International Journal of Nanomedicine*, *3*(3), 311–321.

Rejinold, N. S., Jayakumar, R., & Kim, Y.-C. (2015). Radio frequency responsive nano-biomaterials for cancer therapy. *Journal of Controlled Release*, *204*, 85–97.

Schaue, D., & McBride, W. H. (2015). Opportunities and challenges of radiotherapy for treating cancer. *Nature Reviews Clinical Oncology*, *12*(9), 527–540.

Shakeri-Zadeh, A., Eshghi, H., Mansoori, G. A., & Hashemian, A. R. (2016). Gold nanoparticles conjugated with folic acid using mercaptohexanol as the linker. *Journal Nanotechnology Progress International*, *1*, 13–23.

Shakeri-Zadeh, A., Kamrava, K., Farhadi, M., Hajikarimi, Z., Maleki, S., & Ahmadi, A. (2014). A scientific paradigm for targeted nanophotothermolysis: The potential for nanosurgery of cancer. *Lasers in Medical Science*, *29*(2), 847–853.

Song, G., Cheng, L., Chao, Y., Yang, K., & Liu, Z. (2017). Emerging nanotechnology and advanced materials for cancer radiation therapy. *Advanced Materials*, *29*(32), 1700996.

Spirou, S., Costa Lima, S., Bouziotis, P., Vranješ-Djurić, S., Efthimiadou, E., Laurenzana, A., … Jankovic, D. (2018). Recommendations for in vitro and in vivo testing of magnetic nanoparticle hyperthermia combined with radiation therapy. *Nanomaterials*, *8*(5), 306.

Thapa, R., Galoforo, S., Kandel, S. M., El-dakdouki, M. H., Wilson, T. G., Huang, X., … Wilson, G. D. (2015). Radiosensitizing and hyperthermic properties of hyaluronan conjugated, dextran-coated ferric oxide nanoparticles: Implications for cancer stem cell therapy. *Journal of Nanomaterials*, *16*(1), 400–411.

Wilhelm, C., Fortin, J.-P., & Gazeau, F. (2007). Tumour cell toxicity of intracellular hyperthermia mediated by magnetic nanoparticles. *Journal of Nanoscience and Nanotechnology*, *7*(8), 2933–2937.

Zhang, A.-W., Guo, W.-H., Qi, Y.-F., Wang, J.-Z., Ma, X.-X., & Yu, D.-X. (2016). Synergistic effects of gold nanocages in hyperthermia and radiotherapy treatment. *Nanoscale Research Letters*, *11*(1), 279.

Zhang, X., Xing, J. Z., Chen, J., Ko, L., Amanie, J., Gulavita, S., … Roa, W. (2008). Enhanced radiation sensitivity in prostate cancer by gold-nanoparticles. *Clinical & Investigative Medicine*, *31*(3), 160–167.

Zheng, W., Rong, Z., Gao, F., Cai, Y., Zhou, J., Chen, X., … Tang, J. (2016). Folate-conjugated magnetic nanoparticles for tumor hyperthermia therapy: In vitro and in vivo studies. *Journal of Nanoscience and Nanotechnology*, *16*(8), 8352–8359.

How to cite this article: Hadi F, Tavakkol S, Laurent S, et al. Combinatorial effects of radiofrequency hyperthermia and radiotherapy in the presence of magneto-plasmonic nanoparticles on MCF-7 breast cancer cells. *J Cell Physiol*. 2019;1–8. https://doi.org/10.1002/jcp.28599